MICHIGAN STATE UNIVERSITY

CYCLOTRON LABORATORY

SIMULTANEOUS ANALYSIS OF MAGNETIC MOMENTS AND ELASTIC MAGNETIC ELECTRON SCATTERING FORM FACTORS

B.A. BROWN, R. RADHI and B.H. WILDENTHAL

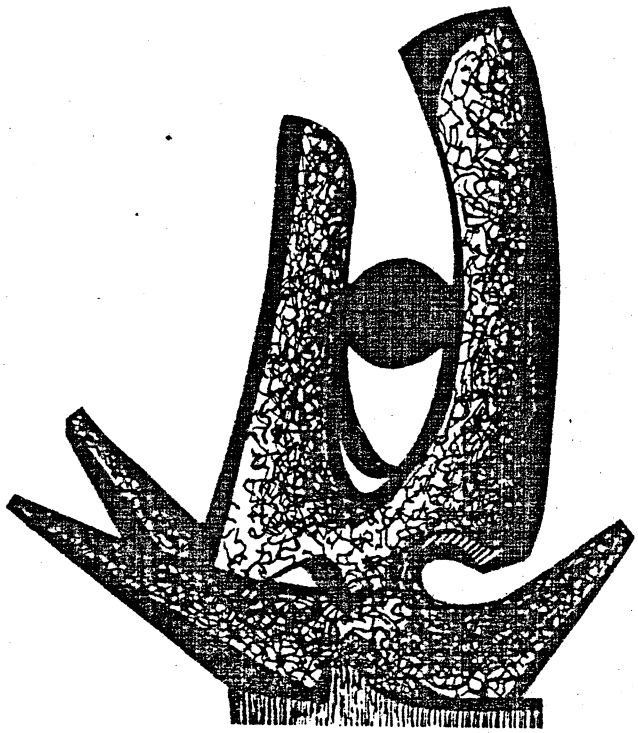

JUNE 1983

MSUCL-423

MSUCL-423
June 1983

Simultaneous analysis of magnetic moments and elastic magnetic electron scattering form factors

B. A. Brown, R. Radhi and B. H. Wildenthal
National Superconducting Cyclotron Laboratory
East Lansing, MI 48824

Abstract: Analysis of the magnetic dipole moments and the elastic magnetic electron scattering form factors of the 1/2+ ground states of ^{19}F, ^{29}Si and ^{31}P demonstrates that the momentum transfer dependence of the data can be understood in terms of a q-independent M1 operator in combination with the effects of configuration mixing within the space of sd-shell orbits.

Elastic magnetic electron scattering form factors are the analogs at non-zero momentum transfers ($q > 0$) of the ($q = 0$) magnetic moments. If the momentum-transfer dependence of the magnetic operator is understood, these scattering data can be combined with the conventional moment to produce an "in depth" picture of a nuclear state. Recently, transverse form factors have been measured for ^{19}F (Ref 1), ^{29}Si and ^{31}P (Ref 2) in the region of momentum transfer $q = 1\text{-}3$ fm^{-1}. Form-factor measurements on these nuclei are of particular interest in that the 1/2+ spin-parities of their ground states rule out excitation of higher multipoles. Hence, the $\Delta J=1$ one-body density matrices of these ground-state wave functions are the only conventional nuclear structure contributions to both the magnetic moments at $q = 0$ and the elastic M1 form-factor values at $q > 0$.

We analyze these data with new mixed-configuration shell-model (CMSM) wave functions. We contrast the results with the consequences of, alternatively, assuming that the wave functions of the nuclear states are those of the simple single-particle shell model (SSPM). The mixed-configuration wave functions we utilise have been obtained in a comprehensive and consistent formulation of the $d_{5/2}$-$s_{1/2}$-$d_{3/2}$ shell model for the nuclei A = 17-39 (Ref 3). These wave functions are derived from the diagonalizations of a single one-body plus two-body Hamiltonian in the

complete sd-shell vector spaces for the chosen combinations of particle number A, isospin T and total angular momentum J. The one-body energies of this Hamiltonian are A-independent and the two-body matrix elements are scaled as $(18/A)^{0.3}$.

The wave functions for ^{19}F, ^{29}Si and ^{31}P obtained in these calculations are used here to evaluate the matrix elements of the $\Delta J=1$ one-body operators $a^{+}(j) \times \tilde{a}(j')$ for the sd-shell orbits $j,j' = d_{5/2}$, $s_{1/2}$ and $d_{3/2}$. These elements of the one-body-density of the multiple-particle shell-model wave functions are the "predictions" for M1 phenomena from the assumed Hamiltonian and model space. When combined with the corresponding single-particle matrix elements and form factors of the M1 operator they yield, respectively, predictions for the magnetic dipole moments and elastic M1 electron scattering. In the present discussions we define the M1 operator to be consistent with the properties of the free neutron and proton and use single particle wave functions of harmonic oscillator form, with size parameters adjusted to be consistent (Ref 4) with the measured rms charge radii of these nuclei.

Our analysis of the magnetic dipole structure of ^{29}Si is presented graphically in Fig. 1. We plot there the predicted and measured absolute values of the magnetic moment and the non-zero-q analogs of this moment obtained from the elastic magnetic electron scattering form factor of ^{29}Si (Ref 2). We use a

representation in Fig. 1 which converts the conventional elastic M1 form factor $F(q)^2$ into a q-dependent magnetic moment

$$\mu(q) = |[F(q)^2 / Q(q)^2]^{1/2}|$$

where

$$Q(q) = \frac{(2)^{1/2}\,\mu_N\,\exp[(-b^2 q^2/4) + (b^2 q^2/4A) - 0.43\,q^2/4]}{(1/q)\exp(-q^6) + (1/q^5)[1 - \exp(-q^6)]}$$

and $\mu_N = 0.1051$ e fm is the nuclear magneton. (The complicated q dependence in the denominator of the equation for Q arises from its being constructed to be of general applicability to cases of mixed M1, M3 and M5 magnetic scattering in the sd shell). At $q = 0$, $\mu(q)$ converges to the conventional definition, modulo the absolute value, of the magnetic moment. At non-zero q values, our representation removes most of the extrinsic exponential q-dependence from the conventional form-factor plot and hence allows us to show both the zero and the non-zero q results in the same linear display. The relationship of theory with experiment is, of course, unchanged by this transformation since at a given value of q both the theoretical and experimental quantities are divided by exactly the same factor.

In Fig. 1 the experimental value of the ^{29}Si magnetic moment is shown as the solid circle on the $q = 0$ axis and the data of Ref 2 are shown as the points in the region $q = 1.2$-2.8 fm^{-1}. The curve in Figure 1 indicated by the symbols "x" shows the SSPM predictions. These are too large by a factor of 4 at $q = 0$ and

too large by a factor, almost constant, of 2 in the region q = 1.2-2.8 fm^{-1}. The solid line in Fig. 1 shows the predictions for the ^{29}Si ground state of the MCSM wave function of Ref 3. With this more realistic wave function the measured value of the moment at q = 0 is well reproduced. The corresponding theoretical values from 1 to 3 fm^{-1} also follow the trend of the experimental data closely, theory systematically being about a factor of 1.2 larger than experiment.

We can understand the mixed-configuration results in terms of interfering contributions to the total q-dependent M1 moment. These contributions come from the expectation values of L and S between the various sd-shell configurations. The L term receives contributions only from the $0d_{5/2}$ and $0d_{3/2}$ orbitals in the present assumption of the free-nucleon M1 operator. The S term receives contributions from both the ℓ =2 orbitals and the $1s_{1/2}$ orbital. These expectation values are weighted by the corresponding g-factors. In Fig. 1 we plot these three separate contributions under the labels g_ℓ (d), g_s (d) and g_s (s), respectively. The three curves combine linearly to give the net q-dependent M1 moment indicated by the solid line.

We see from the curve labeled g_s (s) in Fig. 1, which of course is proportional to the SSPM curve, that one consequence of the configuration mixing is to reduce the contribution of the $1s_{1/2}$

orbit to roughly one half of the single-particle limit. At this level, the $1s_{1/2}$ term alone still gives a q = 0 moment which is a factor of 2 larger than the experimental value. It can be seen that the agreement between the full mixed-configuration prediction and experiment comes about by virtue of cancellation between the g_s (s) term and the g_s (d) term. (The g_ℓ (d) term is practically zero, which is a reflection of the fact that proton excitations in the mixed-configuration ground-state wave function are predicted, somewhat surprisingly, to have virtually no influence on the magnetic moment.)

The contributions of these three terms to the moment are seen from Fig. 1 to depend strongly on q, however, so that the cancellation obtained at q = 0 does not hold at large momentum transfers. In particular, the contribution of the g_s (d) term is seen to drop to zero by q = 1.5 fm^{-1}. This leaves the g_s (s) term as the sole contributor to the total moment throughout most of the region covered in the electron-scattering measurements. In this region, the factor of 2 reduction from the single-particle limit of the contribution of the $1s_{1/2}$ term is in qualitative agreement with observation, as is the q dependence stemming from the the use of the harmonic-oscillator $1s_{1/2}$ single-particle wave function.

We present theoretical predictions for ^{31}P together with experimental data (Ref 2) in Fig. 2. The essential difference between ^{29}Si and ^{31}P is that here we are dealing with a state

which has an odd proton rather than an odd neutron. Hence, the contribution of the g_ℓ (d) term is no longer negligible, although it is still small relative to the spin terms. The relationships between the data, the SSPM results and CMSM predictions are otherwise much the same for ^{31}P as those found for ^{29}Si, thus reinforcing our confidence that our understanding of these phenomena is correct.

Our final example is the case of ^{19}F. We present our calculations in comparison with the data of Ref 1 in Fig. 3. As in the case of ^{31}P we are dealing here with an odd-proton nucleus. However, as can be immediately noticed from Fig. 3, ^{19}F exhibits radically different behavior from that of ^{31}P at q = 0. The value of its magnetic moment at q = 0 has essentially the full single-particle value. Thus, unlike the cases of ^{29}Si and ^{31}P, the SSPM gives a good accounting for the q=0 moment of ^{19}F. At the same the time, the mixed-configuration prediction is in equivalently good agreement with the experimental value. Thus, while configuration mixing has the effect of quenching the predicted q=0 magnetic moments below the SSPM values by factors of 3 to 4 in the A = 31 and 29 cases, it yields a prediction slightly larger than the SSPM value for ^{19}F. It might thus be assumed that the realistic wave function of ^{19}F closely resembles a pure $1s_{1/2}$ proton. However, this is contradicted by the fact that the SSPM predictions are 2 to 3 times larger than either the CMSM predictions or the data in the region q = 1.5-2.5 fm^{-1}.

The quandary posed so far by our discussion of ^{19}F is resolved by reference to the predictions for the same individual L and S contributions which we examined in the cases of ^{29}Si and ^{31}P. As in those instances, we see that for ^{19}F the configuration mixing quenches the $1s_{1/2}$ contribution by about a factor of 2 from the SSPM limit. The critical difference in ^{19}F is that here the g_s (d) contribution has the same, rather than opposite, sign as the g_s (s) term, rather. Hence, all three contributions to the moment at q = 0 add constructively, summing to approximately the SSPM value. Beyond q = 1.5 fm^{-1}, the ℓ =2 contributions, as in the ^{31}P and ^{29}Si cases, drop to essentially zero. In this region the mixed-configuration prediction involves only the $1s_{1/2}$ contribution and, again as for ^{31}P and ^{29}Si, the amount of quenching induced by configuration mixing appears to be in good accord with the electron scattering results.

In summary, the simultaneous analysis of the magnetic dipole moments and elastic form factors for each of the nuclei ^{19}F, ^{29}Si and ^{31}P in the context of the simple single-particle model implies in each case a strong momentum dependence of the effective M1 operator. Moreover, this momentum dependence is found to change drastically from nucleus to nucleus. In ^{19}F a factor of 2 quenching between q = 0 and 2 fm^{-1} is implied, while for ^{31}P and ^{29}Si, a factor of 2 enhancement over the same range is necessary if the SSPM shapes are normalized to the magnetic moment values.

In contrast, analyses of the same data with realistic mixed-configuration shell-model wave functions yield good agreement for all three nuclei over all momentum transfers. This is obtained with a momentum-transfer-independent formulation of the M1 operator normalized to the free-nucleon g-factors. In these analyses, all of the observed variation of the magnetic moments with respect to q originates from mixings of the three sd-shell orbitals and the differing dependences of their individual moments upon q. The present analyses clearly demonstrate the coupling between the formulation of the effective M1 operator and the description of nuclear wave functions. The mixed-configuration wave functions are complex and account for many details of nuclear structure with quantitative accuracy. Complementarily, they are consistent with a very simple formulation of the M1 operator. In this context we note that there is the suggestion from the present analyses that the $1s_{1/2}$ matrix element of the effective M1 spin operator is quenched below the free-nucleon normalization by a factor of 0.8-0.9.

Acknowledgments

We are grateful to H. Miessen, H. Rothhaas and C. Williamson and their collaborators for providing their experimental data prior to publication and to A. E. L. Dieperink and B. Frois for stimulating discussions of thes problem. This research was supported in part by the National Science Foundation grant no. PHY-80-17605.

Figure captions

Figure 1: The momentum-dependent magnetic moment $\mu(q)$ for ^{29}Si. The arrow points to the experimental magnetic moment (Ref 5) at q=0. The values plotted at non-zero values of q are values of $\mu(q) = |F^2(q)/Q^2(q)|^{1/2}$, where $F^2(q)$ is the transverse magnetic form factor and $Q^2(q)$ is the conversion factor defined in the text. The experimental data Ref 2, obtained at the MIT-Bates (circles) and Mainz (triangles) accelerators, are plotted as functions of q_{eff}. The theoretical values of $\mu(q)$, calculated in the PWBA, are plotted as functions of q. Results are shown for a pure $2s_{1/2}$ single-particle wave function (crosses) and for the full $(sd)^n$ wave function (solid line). These results were obtained with the use of free-nucleon g factors and harmonic-oscillator radial wave functions with b = 1.825 fm. The decomposition of the full curve is shown for the individual contributions from the magnetization current due to the 1s orbit [the dotted line labled $g_s(s)$], the magnetization current due to the 0d orbit [the dashed curve labeled $g_s(d)$] and the convection current due to the 0d orbit [the dot-dashed curve labeled $g_\ell(d)$].

Figure 2: The momentum-dependent magnetic moment $\mu(q)$ for ^{31}P. The experimental points Ref 2 and theoretical curves (with b=1.848 fm) are presented with the same conventions described in the caption to Figure 1.

Figure 3: The momentum-dependent magnetic moment $\mu(q)$ for ^{19}F. The experimental points Ref 1 and theoretical curves (with b=1.833 fm) are presented with the same conventions described in the caption to Figure 1.

References:

1. C.F. Williamson, S. Kowalski, F.N. Rad, J. Heisenberg, H. Crannell and J.T. O'Brien, private communication, 1983.

2. H. Miessen, Ph.D. Thesis, Johannes Gutenberg University, Mainz, 1982; H. Miessen, G. Luehrs, H. Rothhaas, W. Bertozzi, S. Kowalski, C.F. Williamson, R.S. Hicks, R.A. Lindgren, G.A. Peterson and B.L. Berman, private communication, 1983.

3. B.H. Wildenthal, Bull. Am Phys. Soc. 27, 725 (1982).

4. B.A. Brown, W. Chung and B.H. Wildenthal, Phys. Rev. C22, 774 (1980).

5. P.M. Endt and C. van der Leun, Nucl. Phys. A310, 1 (1978).

MSU-83-272

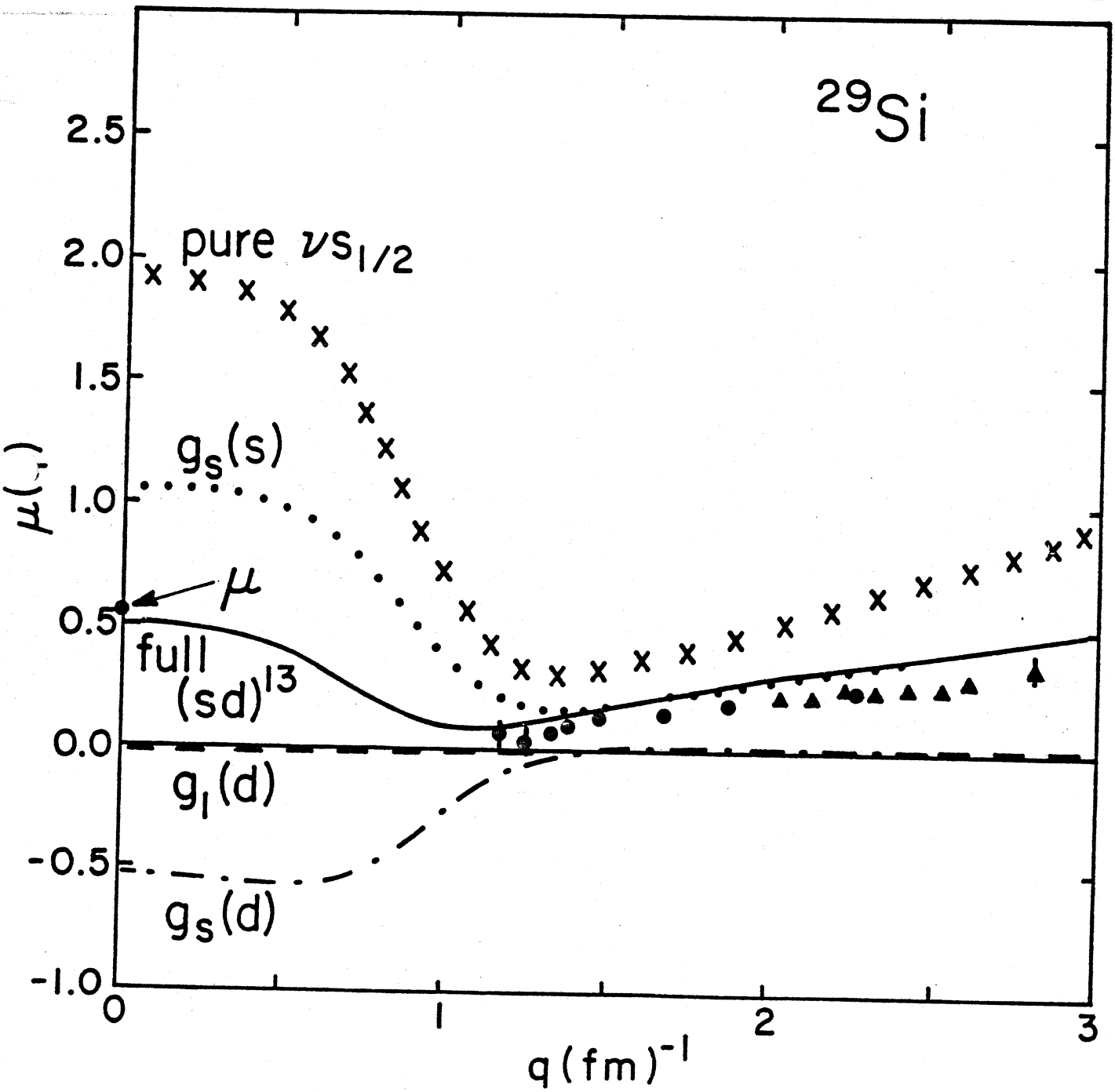

Fig. 1

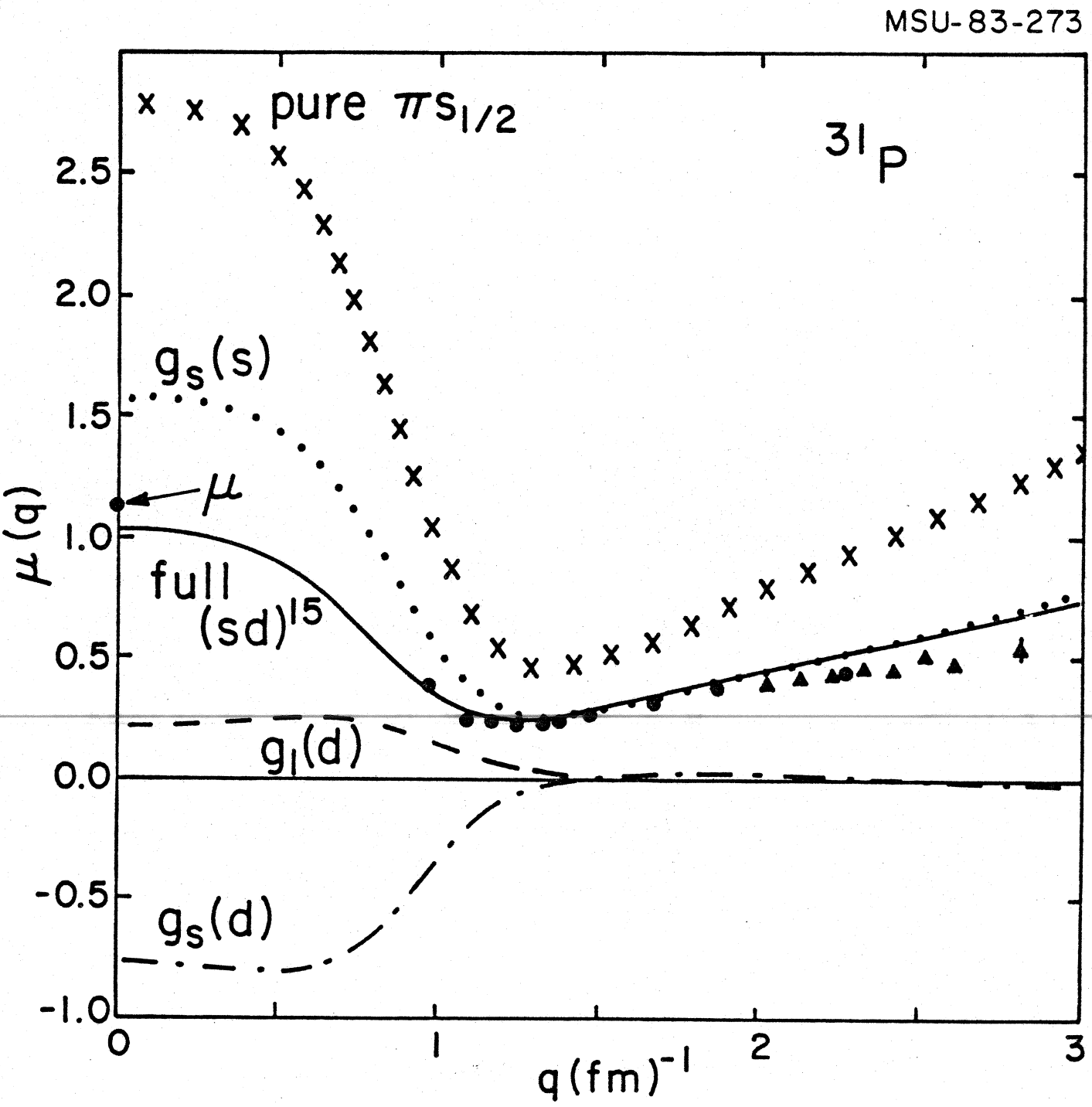
MSU-83-273
x x x pure $\pi s_{1/2}$
^{31}P
$g_s(s)$
μ
full
$(sd)^{15}$
$g_l(d)$
$g_s(d)$
$\mu(q)$
$q(fm)^{-1}$
2.5
2.0
1.5
1.0
0.5
0.0
-0.5
-1.0
0
1
2
3

Fig. 2

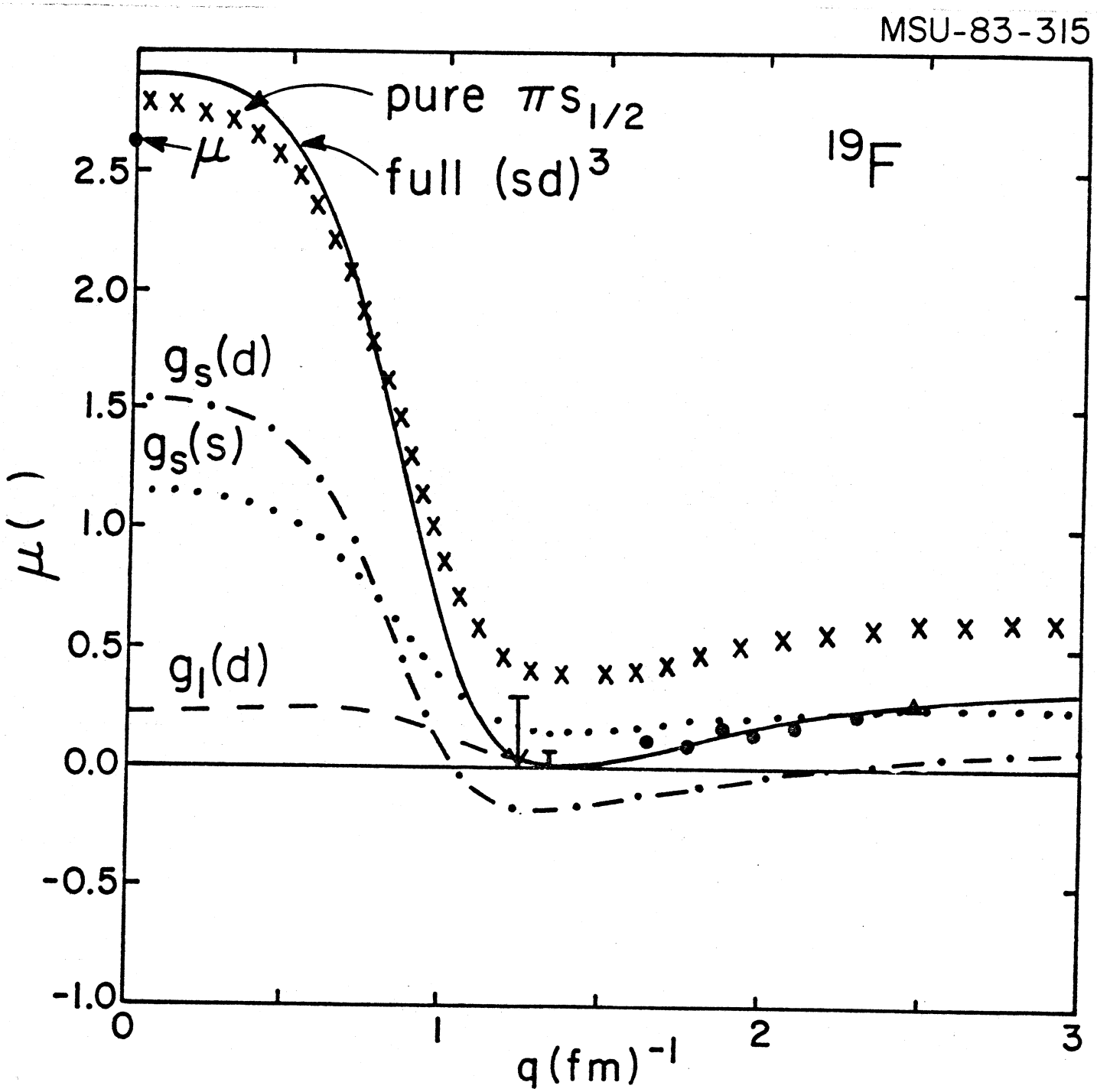
MSU-83-315
pure $\pi s_{1/2}$
full $(sd)^3$
^{19}F
μ
$g_s(d)$
$g_s(s)$
$g_l(d)$
$\mu(\ )$
2.5
2.0
1.5
1.0
0.5
0.0
-0.5
-1.0
0
1
2
3
$q(fm)^{-1}$

Fig. 3